Fluorescent Probes

DOI: 10.1002/ange.201407181

# High-Throughput Development of a Hybrid-Type Fluorescent Glutamate Sensor for Analysis of Synaptic Transmission**

*Kenji Takikawa, Daisuke Asanuma, Shigeyuki Namiki, Hirokazu Sakamoto, Tetsuro Ariyoshi, Naoya Kimpara, and Kenzo Hirose**

***Abstract:*** *Fluorescent sensors are powerful tools for visualizing cellular molecular dynamics. We present a high-throughput screening system, designated hybrid-type fluorescence indicator development (HyFInD), to identify optimal position-specific fluorophore labeling in hybrid-type sensors consisting of combinations of ligand-binding protein mutants with small molecular fluorophores. We screened sensors for glutamate among hybrid molecules obtained by the reaction of four cysteine-reactive fluorescence probes with a set of cysteine-scanning mutants of the 274 amino acid S1S2 domain of AMPA-type glutamate receptor GluA2 subunit. HyFInD identified a glutamate-responsive probe (enhanced glutamate optical sensor: eEOS) with a dynamic range >2400%, good photostability, and high selectivity. When eEOS was specifically tethered to neuronal surfaces, it reliably visualized the spatiotemporal dynamics of glutamate release at single synapses, revealing synapse-to-synapse heterogeneity of short-term plasticity.*

Synaptic transmission mediated by glutamate is an elementary process in information processing in the brain, and its modulation is thought to be important for high-order brain functions.[1] Nevertheless, the modulation of synaptic transmission remains poorly understood because of the lack of proper tools for investigation. For example, several fluorescent glutamate sensors, including FLIPE,[2] EOS,[3,4] SuperGluSnFR,[5] and Snifit-iGluR5,[6] have been developed for glutamate imaging, but have severe limitations for visualizing synaptic glutamate dynamics, mainly because of their low dynamic ranges (up to about 50% on neuronal surfaces). A recent GFP-based sensor iGluSnFR[7] showed a moderate dynamic range (ca. 100% on neuronal surfaces), but its inadequate photostability and strong pH-dependence, because of the intrinsic nature of the GFP fluorophore, are considerable drawbacks for the imaging of synaptic glutamate.

To develop suitable glutamate sensors for visualizing synaptic transmission, we focused on hybrid-type fluorescent sensors consisting of a ligand-binding protein and a small molecular fluorophore (Figure 1a), which can inherit the good properties of the ligand-binding proteins (e.g. ligand selectivity) and the labeling fluorophores (e.g. photostability and pH-insensitivity). To efficiently identify sensors with a high dynamic range for high signal-to-noise ratio imaging among large numbers of candidate hybrids, we constructed a high-throughput system for sequence-scanning screening of fluorophore labeling positions, which we designate as hybrid-type fluorescence indicator development (HyFInD; Figure 1b, see also the Supporting Information). Briefly, cys-

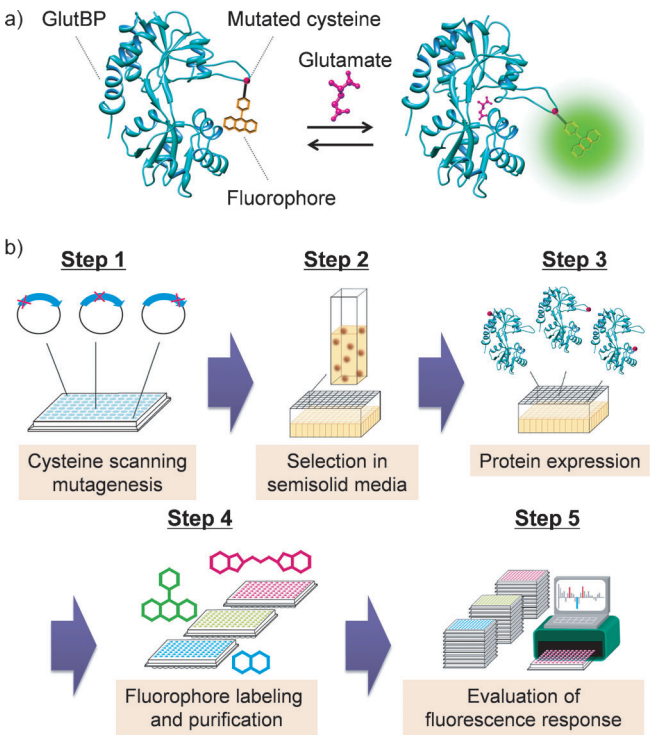


***Figure 1.*** HyFInD screening for hybrid-type glutamate sensors. a) Schematic illustration of a hybrid-type glutamate sensor consisting of a GlutBP and a fluorophore. The fluorophore attached to the site of an engineered cysteine residue on GlutBP senses the conformational change in the protein induced by glutamate binding, and this results in a change in the fluorescence intensity when the fluorophore is positioned appropriately. b) The HyFInD screening system. The system is based on a 96-well plate format procedure, the entire processes of which can be completed within one week.

[*] Dr. K. Takikawa, Dr. D. Asanuma, Dr. S. Namiki, H. Sakamoto, T. Ariyoshi, N. Kimpara, Prof. K. Hirose
Graduate School of Medicine, The University of Tokyo
7-3-1 Hongo, Bunkyo-ku, Tokyo (Japan)
E-mail: kenzoh@m.u-tokyo.ac.jp

[**] We thank S. Iinuma and M. Kanda for their participation during the preliminary stage of this study. This work was supported in part by grants from SENTAN, JST (to K.H.), the Strategic Research Program for Brain Sciences, MEXT (to K.H.), KAKENHI (Grant no. 11J05563 to K.T., 26560441 to D.A., 24115502, 24590313, and 25115704 to S.N., and 24116004 to K.H.), and Research Foundation for Opto-Science and Technology (to D.A.)

Supporting information for this article (including detailed experimental procedures) is available on the WWW under http://dx.doi.org/10.1002/anie.201407181.

teine-scanning mutagenesis produced a set of mutant glutamate-binding proteins (GlutBPs; 274 amino acids) derived from the S1S2 domain of the AMPA-type glutamate receptor GluA2 subunit[8] (see Figure S1a in the Supporting Information). Labeling of these mutants with cysteine-reactive fluorophores generated an array of fluorescent conjugates, and their fluorescence responses to glutamate were evaluated. By using the HyFInD system, we screened 1080 combinations of 270 species of cysteine-mutagenized GlutBPs and 4 commercially available fluorophores, that is, Alexa Fluor 350 (AX350), Oregon Green (OG), Alexa Fluor 488 (AX488), and Cy3 (see Figure S1b in the Supporting Information). We identified 28 hit conjugates (2.6% of the total) presenting a change in the fluorescence of not less than 20% upon addition of glutamate (Figure 2). AX488 was particularly notable among the four fluorophores, being a component of 14 sensors that showed generally high fluorescence responses of up to about 350%. Therefore, we focused on the AX488-based hybrid-type sensors.

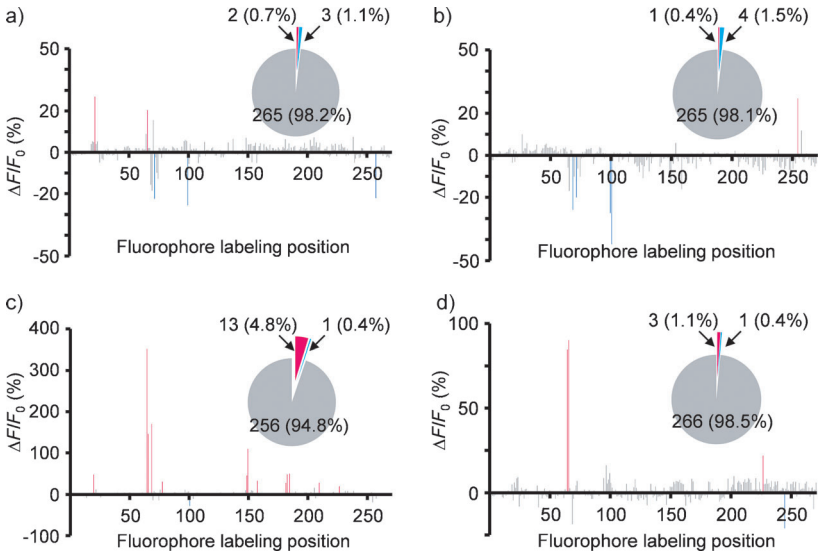


***Figure 2.*** Results of HyFInD screening. Fluorescence changes in the fluorescent GlutBP conjugates with a) OG, b) Cy3, c) AX488, and d) AX350. Bars represent percent changes in fluorescence intensity ($\Delta F/F_0$, %) upon addition of glutamate (final 2 mM). Red and blue bars indicate >20% increase and decrease in fluorescence intensity, respectively. Gray bars represent others. The horizontal axes indicate the positions of fluorophore labeling, where the numbers 1 to 270 correspond to the residue numbers of GlutBP 383–775, excluding endogenous cysteine residues (see Figure S1 in the Supporting Information). Inset: In the pie charts, red and blue represent the proportions of fluorescent conjugates showing a >20% increase and decrease, respectively, in the fluorescence intensity upon addition of glutamate. Gray represents the others.

In HyFInD screening, we used a mixture of structural 5,6-isomers of AX488 as a labeling fluorophore (see Figure S1b in the Supporting Information). Thus, we first investigated whether the structural AX488 isomers have different effects on the fluorescence response of the sensors. We purified the 5/6-isomers (denoted as AX488 I/II, respectively), and further screened 28 conjugates prepared by labeling the 14 identified GlutBPs with each isomer. Intriguingly, the choice of the labeling dye resulted in dramatic differences in the fluorescence response of the sensors (see Figure S2 in the Supporting Information), although free AX488 I and II have similar photochemical properties (see Table S1 in the Supporting Information); for example, N461C-AX488 I showed a 290% change, whereas N461C-AX488 II showed almost no change.

The synaptic glutamate concentration is estimated to be of submicromolar levels in the extracellular space in the resting state,[9,10] but can be transiently increased up to millimolar levels in the synaptic cleft[11] and to micromolar levels in the extracellular space around synapses[4] upon synaptic transmission. We thus set a criterion of several tens of micromolar orders of magnitude of glutamate affinity for the selection of sensors. For the AX488-based sensors, we estimated $EC_{50}$ values based on a screening-format titration and found that these values ranged from submicromolar to submillimolar order (see Table S2 in the Supporting Information), thus varying greatly from the affinity of the original GlutBP ($K_d$ = 0.55 μM).[12] This kind of affinity shift often occurs upon labeling ligand-binding proteins with fluorophores.[13] Among the candidates, we selected G448C-AX488 II (named eEOS) as a promising sensor for visualizing synaptic glutamate dynamics from the viewpoints of both $EC_{50}$ value (66 μM) and dynamic range (>700%).

To more precisely characterize eEOS, we further purified eEOS by ion-exchange chromatography and found that it exhibits an extremely large change in fluorescence (>2400%) upon glutamate addition (Figure 3a); the fluorescence quantum yield (QY) dynamically increased from 0.045 to 0.82, which is almost equivalent to that of free AX488 (QY = 0.92; see Table S1 in the Supporting Information). The addition of glutamate caused almost no change in the absorbance maximum, but induced a slight blue shift of the absorption maximum of eEOS (500 nm to 496 nm), which approximates to that of free AX488 ($\lambda_{abs,max}$ = 494 nm, Figure 3a; see also Table S1 in the Supporting Information).

We confirmed the L-glutamate-sensing selectivity of eEOS over other amino acid neuro/gliotransmitters (L-aspartate, glycine, GABA, and D-serine) and structurally similar amino acids (D-glutamate and L-glutamine, Figure 3b). This L-glutamate selectivity of eEOS was likely a consequence of the choice of GlutBP. We also analyzed the association and dissociation kinetics between eEOS and glutamate by means of stopped-flow fluorescence measurements, and determined that the $k_{on}$ and $k_{off}$ values were $1.2\times10^5\,M^{-1}s^{-1}$ and $1.4\times10\,s^{-1}$, respectively (see Figure S3a,b in the Supporting Information).

We found that eEOS is highly photostable, whereas a control GFP-based sensor, iGluSnFR, showed strange fall-and-rise kinetics of the fluorescence, which might arise from the photoconvertible nature of GFP[14] (see Figure S3c in the Supporting Information). Moreover, eEOS showed an almost

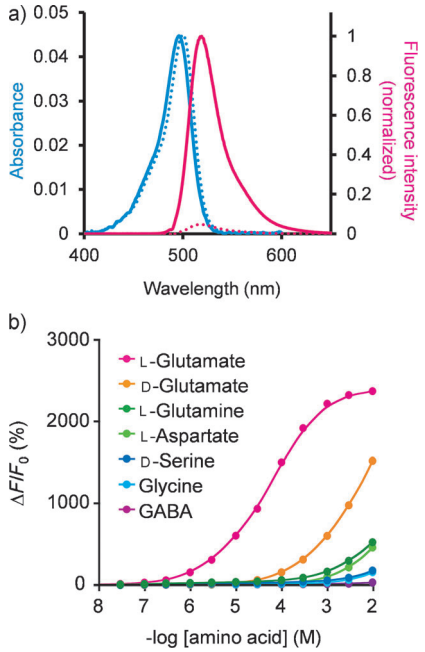


***Figure 3.*** In vitro properties of eEOS. a) Absorbance spectra (blue) and normalized fluorescence emission spectra (pink) profiles of eEOS with (solid line) or without 10 mM L-glutamate (dashed line). b) Titration curves of eEOS with L-glutamate and other amino acids.

constant fluorescence intensity between pH 5.0 and 8.0 in the presence or the absence of glutamate, whereas iGluSnFR showed a large pH-dependent change in the fluorescence emission, likely because of the pH-sensitive nature of the GFP fluorophore[7,15] (see Figure S3d in the Supporting Information). The pH insensitivity of eEOS is favorable for the reliable monitoring of synaptic glutamate dynamics, because extracellular pH changes are well-known to accompany neural activity.[16]

To visualize glutamate dynamics in neurons, we targeted eEOS to neurons by means of biotin-streptavidin-assisted conjugation to BoNT/C-Hc, which is a nontoxic carboxy-terminal domain of the heavy chain of the *Clostridium botulinum* type C neurotoxin, which binds to neuronal surface gangliosides GD1b and GT1b[17] (Figure 4a). By simply adding this complex to a neuron-astrocyte coculture system, we achieved specific eEOS labeling of the neuronal surfaces, without nonspecific staining of astrocytes (see Figure S4a in the Supporting Information). We found that the dissociation constant for glutamate with eEOS bound on the neuronal surface was 50.3 μM, which is almost identical to that of free eEOS ($K_d = 41.6$ μM), and bound eEOS showed a much higher dynamic range (ca. 500%) than iGluSnFR (ca. 100%).[7] Moreover, bound eEOS showed good photostability, whereas iGluSnFR did not (see Figure S4b,c in the Supporting Information). These results demonstrate that eEOS has suitable properties for monitoring glutamate dynamics in situ.

We next examined whether eEOS could be used to visualize action potential (AP) evoked glutamate release at the level of a single synapse. Single-field electrical stimulation elicited rapid changes in the eEOS fluorescence, which appeared as discrete hot spots along the dendrite and spatially corresponded to the immunoreactivity of the glutamatergic presynaptic terminal marker vesicular glutamate transporter-1 (VGLUT1; Figure 4b). The fluorescence changes returned to the baseline level with a time constant of 0.17 s (Figure 4c). Furthermore, changes in the eEOS fluorescence in response to electrical stimulation were never observed when extracellular $Ca^{2+}$ was omitted (Figure 4b,c), thereby confirming that the observed fluorescence change was a result of $Ca^{2+}$-dependent vesicular glutamate release.[18] The addition of phorbol 12-myristate 13-acetate (PMA) tended to increase the AP-evoked changes in eEOS fluorescence at individual synapses (Figure 4a,b and see Figure S5 in the Supporting Information). This result is in line with the fact that the efficacy of vesicular release is enhanced by phorbol esters,[19] which suggests that eEOS reliably detects changes in the amount of glutamate released at synapses.

The efficacy of neurotransmitter release rapidly increases or decreases during repetitive neuronal activity, a phenomenon that is known as short-term synaptic plasticity,[20] which plays important roles in information processing in the brain.[1] We therefore examined whether short-term plasticity of glutamate release can be evaluated by using eEOS. We compared single AP-evoked changes in eEOS fluorescence elicited by two different stimulation frequencies, 0.1 Hz and 20 Hz (Figure 4d). We found that some synapses showed facilitation at 20 Hz stimulation, while other synapses showed depression. Our analysis revealed that short-term plasticity (the degree of facilitation or depression) was heterogeneous among synapses formed on the same dendrite, even between neighboring synapses (Figure 4d).

To examine the molecular mechanisms underlying the fluorescence modulation of AX488-based sensors, we also performed multivariate logistic regression analysis, focusing on the relationship between the hit positions of fluorophore labeling and the surrounding arrangement of amino acids. As quantitative explanatory variables, we adopted 1) the degree of local conformational change around the fluorophore-labeling position and 2) the distances from the labeling position to each kind of amino acid residing closest to the labeling position. Model selection was based on Akaike's information criterion (AIC; see the Supporting Information). In the optimal model, hit occurrence was dependent not only on local conformational changes, but also on the distance from the nearest lysine and tryptophan residues (see Table S3 in the Supporting Information). From the viewpoint of interactions between the amino acids and the fluorophore, although lysine has no apparent effect on AX488 fluorescence (see Figure S6 in the Supporting Information), it possesses a positively charged side chain and we speculate that lysine in proximity to negatively charged AX488 would electrostatically attract the dye, thereby blocking photochemical interaction with the surroundings, for example, fluorescence quenching. On the other hand, tryptophan strongly quenches the fluorescence of certain fluorophores[21–23] including AX488[24] ($K_{SV} = 36.5\ M^{-1}$; see Figure S6 in the Supporting Information). By using such quenching, Neuweiler et al. have developed a fluorophore-peptide-based sensor for p53 autoantibodies.[25] Tryptophan-induced

  

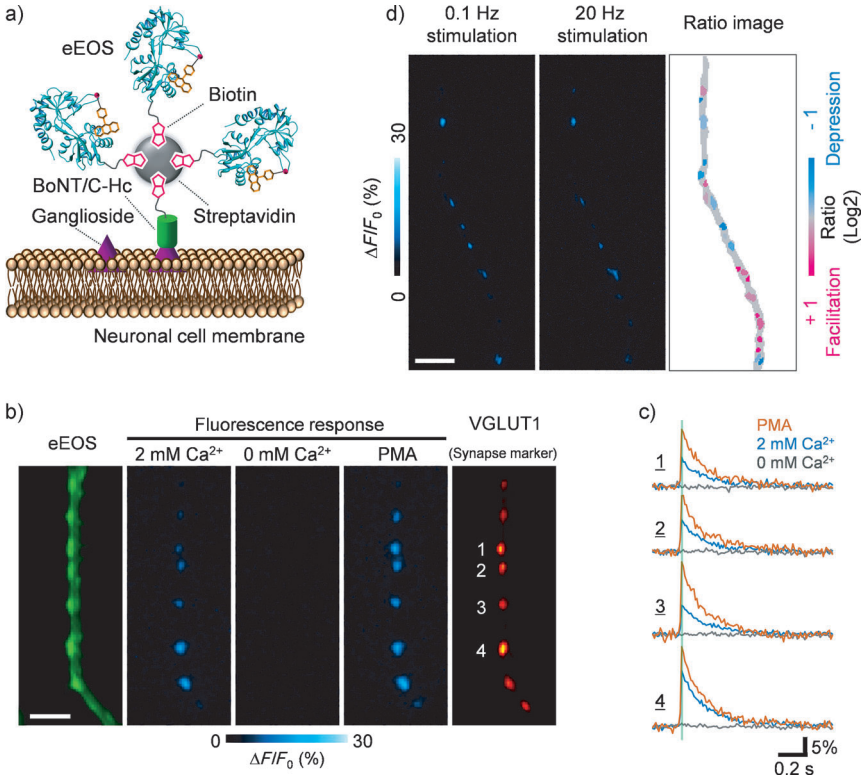


***Figure 4.*** Glutamate imaging at a single-synapse level using eEOS. a) Schematic illustration of eEOS labeling of the neuronal cell surface. eEOS is anchored by BoNT/C-Hc, which binds to neuronal surface gangliosides. b) Fluorescence image of eEOS anchored on the neuronal cell membrane via BoNT/C-Hc (left, green). Averaged images of fluorescence responses ($\Delta F/F_0$, %) of eEOS evoked by a single electrical stimulation in the presence of 2 mM $Ca^{2+}$ (middle left, cyan), 0 mM $Ca^{2+}$ (middle, cyan), and PMA (middle right, cyan) in extracellular saline, and an immunofluorescence image of VGLUT1 (right, red) are shown. Scale bar: 5 μm. c) Time courses of AP-evoked changes in eEOS fluorescence ($\Delta F/F_0$, %) at 4 individual synapses in (b) in the presence of 2 mM $Ca^{2+}$ (blue), 0 mM $Ca^{2+}$ (gray), and PMA (orange) in extracellular saline. A green vertical line represents the timing of single-field electrical stimulation. Each time trace was the average of 15 trials, except for the PMA traces (average of 5 trials). d) Images of representative fluorescence responses ($\Delta F/F_0$, %) of eEOS (averaged from 40 trials) evoked by 0.1 Hz (left) or 20 Hz (middle) stimulation. The right image shows the ratio of fluorescence changes of eEOS in response to 0.1 Hz and 20 Hz stimulation. Scale bar: 10 μm.

quenching might similarly underlie the glutamate-dependent fluorescence change of our sensor.

The HyFInD system enabled rapid sequence-scanning screening (we achieved a processing rate of > 1000 conjugates a week) and provided a variety of sensors, from which we selected eEOS as a suitable sensor. Statistical analysis provided clues as to the mechanism of the change in the fluorescence of the sensors, which might be helpful for the rational molecular design of sensors. However, since even slight structural differences in the labeling fluorophores can drastically influence ligand affinity and the dynamic range, as seen in the GlutBP-AX488 I/II conjugates, the HyFInD approach should be a useful tool for the development of optimal sensors.

The identified eEOS has a wide dynamic range (> 2400 %), good photostability, pH insensitivity, and high glutamate selectivity. The sensor is not ratiometric, thus precluding the use for the direct quantification of absolute glutamate levels. Instead, eEOS finds great applicability in sensitively detecting time-dependent subtle changes in relative glutamate levels. Indeed, eEOS enabled the functional imaging of glutamate release at single synapses, successfully revealing the heterogeneity of synaptic short-term plasticity. Previously, when applied by direct injection to rat brain slices and in vivo rat somatosensory cortex, our prototype EOS properly functioned as a glutamate sensor.[4] Thus, we plan to visualize ex vivo/in vivo glutamate dynamics with eEOS for analyzing synaptic transmission in neuronal circuits.

We anticipate that the HyFInD approach with appropriate choices of ligand-binding proteins and labeling fluorophores will enable the development of sensors for many molecules of interest. The choice of protein is not limited to endogenous receptor proteins, because, for example, the single-chain variable fragment (scFv),[26,27] monobody,[28] and designed ankyrin repeat proteins (e.g. DARPins)[29] can also serve as ligand-binding proteins. In addition, the flexibility in the choice of the fluorophore should make it possible to obtain a range of sensors with different colors, which would be useful for multiple molecular imaging. As another possibility, the selection of far-red to near-infrared fluorophores such as MR121 and ATTO 655, which are quenched quite efficiently by tryptophan,[21–23,25] might afford sensors, similar to AX488, suitable for in vivo deep-tissue imaging. We are currently using HyFInD to develop other hybrid-type sensors for precise spatiotemporal imaging of a range of molecular targets.

Received: July 14, 2014
Published online: October 8, 2014

**Keywords:** fluorescent probes · high-throughput screening · neurotransmitters

[1] L. F. Abbott, W. G. Regehr, *Nature* **2004**, *431*, 796–803.
[2] S. Okumoto, L. L. Looger, K. D. Micheva, R. J. Reimer, S. J. Smith, W. B. Frommer, *Proc. Natl. Acad. Sci. USA* **2005**, *102*, 8740–8745.
[3] S. Namiki, H. Sakamoto, S. Iinuma, M. Iino, K. Hirose, *Eur. J. Neurosci.* **2007**, *25*, 2249–2259.
[4] Y. Okubo, H. Sekiya, S. Namiki, H. Sakamoto, S. Iinuma, M. Yamasaki, M. Watanabe, K. Hirose, M. Iino, *Proc. Natl. Acad. Sci. USA* **2010**, *107*, 6526–6531.
[5] S. A. Hires, Y. Zhu, R. Y. Tsien, *Proc. Natl. Acad. Sci. USA* **2008**, *105*, 4411–4416.
[6] M. A. Brun, K.-T. Tan, R. Griss, A. Kielkowska, L. Reymond, K. Johnsson, *J. Am. Chem. Soc.* **2012**, *134*, 7676–7678.

[7] J. S. Marvin, B. G. Borghuis, L. Tian, J. Cichon, M. T. Harnett, J. Akerboom, A. Gordus, S. L. Renninger, T.-W. Chen, C. I. Bargmann, M. B. Orger, E. R. Schreiter, J. B. Demb, W.-B. Gan, S. A. Hires, L. L. Looger, *Nat. Methods* **2013**, *10*, 162 – 170.
[8] G. Q. Chen, Y. Sun, R. Jin, E. Gouaux, *Protein Sci.* **1998**, *7*, 2623 – 2630.
[9] N. Zerangue, M. P. Kavanaugh, *Nature* **1996**, *383*, 634 – 637.
[10] M. A. Herman, C. E. Jahr, *J. Neurosci.* **2007**, *27*, 9736 – 9741.
[11] J. D. Clements, R. A. Lester, G. Tong, C. E. Jahr, G. L. Westbrook, *Science* **1992**, *258*, 1498 – 1501.
[12] R. Abele, K. Keinanen, D. R. Madden, *J. Biol. Chem.* **2000**, *275*, 21355 – 21363.
[13] R. M. de Lorimier, J. J. Smith, M. A. Dwyer, L. L. Looger, K. M. Sali, C. D. Paavola, S. S. Rizk, S. Sadigov, D. W. Conrad, L. Loew, H. W. Hellinga, *Protein Sci.* **2002**, *11*, 2655 – 2675.
[14] G. H. Patterson, J. Lippincott-Schwartz, *Science* **2002**, *297*, 1873 – 1877.
[15] R. Y. Tsien, *Annu. Rev. Biochem.* **1998**, *67*, 509 – 544.
[16] M. Chesler, *Physiol. Rev.* **2003**, *83*, 1183 – 1221.
[17] K. Tsukamoto, T. Kohda, M. Mukamoto, K. Takeuchi, H. Ihara, M. Saito, S. Kozaki, *J. Biol. Chem.* **2005**, *280*, 35164 – 35171.
[18] R. Jahn, D. Fasshauer, *Nature* **2012**, *490*, 201 – 207.
[19] R. C. Malenka, D. V. Madison, R. A. Nicoll, *Nature* **1986**, *321*, 175 – 177.
[20] R. S. Zucker, W. G. Regehr, *Annu. Rev. Physiol.* **2002**, *64*, 355 – 405.
[21] N. Marmé, J.-P. Knemeyer, M. Sauer, J. Wolfrum, *Bioconjugate Chem.* **2003**, *14*, 1133 – 1139.
[22] S. Doose, H. Neuweiler, M. Sauer, *ChemPhysChem* **2005**, *6*, 2277 – 2285.
[23] S. Doose, H. Neuweiler, M. Sauer, *ChemPhysChem* **2009**, *10*, 1389 – 1398.
[24] H. Chen, S. S. Ahsan, M. B. Santiago-Berrios, H. D. Abruña, W. W. Webb, *J. Am. Chem. Soc.* **2010**, *132*, 7244 – 7245.
[25] H. Neuweiler, A. Schulz, A. C. Vaiana, J. C. Smith, S. Kaul, J. Wolfrum, M. Sauer, *Angew. Chem. Int. Ed.* **2002**, *41*, 4769 – 4773; *Angew. Chem.* **2002**, *114*, 4964 – 4968.
[26] M. Renard, L. Belkadi, N. Hugo, P. England, D. Altschuh, H. Bedouelle, *J. Mol. Biol.* **2002**, *318*, 429 – 442.
[27] R. Abe, H. Ohashi, I. Iijima, M. Ihara, H. Takagi, T. Hohsaka, H. Ueda, *J. Am. Chem. Soc.* **2011**, *133*, 17386 – 17394.
[28] A. Gulyani, E. Vitriol, R. Allen, J. Wu, D. Gremyachinskiy, S. Lewis, B. Dewar, L. M. Graves, B. K. Kay, B. Kuhlman, T. Elston, K. M. Hahn, *Nat. Chem. Biol.* **2011**, *7*, 437 – 444.
[29] L. Kummer, C.-W. Hsu, O. Dagliyan, C. MacNevin, M. Kaufholz, B. Zimmermann, N. V. Dokholyan, K. M. Hahn, A. Plückthun, *Chem. Biol.* **2013**, *20*, 847 – 856.

  